Developmental Cell, Vol. 6, 815–829, June, 2004, Copyright ©2004 by Cell Press

Cell Cycle Control of Kinesin-Mediated Transport of Bik1 (CLIP-170) Regulates Microtubule Stability and Dynein Activation

Pedro Carvalho,[1,2] Mohan L. Gupta, Jr.,[1] M. Andrew Hoyt,[3] and David Pellman[1,*]

[1]Department of Pediatric Oncology, Dana-Farber Cancer Institute and Division of Hematology/Oncology
Children's Hospital Boston and Harvard Medical School
Boston, Massachusetts 02115
[2]Institute for Biomedical Sciences Abel Salazar
4099-003 Porto
Portugal
[3]Department of Biology
Johns Hopkins University
Baltimore, Maryland 21218

Summary

CLIPs are microtubule plus end-associated proteins that mediate interactions required for cell polarity and cell division. Here we demonstrate that budding yeast Bik1, unlike its human ortholog CLIP-170, is targeted to the microtubule plus end by a kinesin-dependent transport mechanism. Bik1 forms a complex with the kinesin Kip2. Fluorescently labeled Bik1 and Kip2 comigrate along individual microtubules. Bik1 exists in distinct intracellular pools: a stable pool at the spindle pole body that is depleted during cell cycle progression, a soluble pool from which Bik1 can be recruited during microtubule initiation, and a dynamic plus end pool maintained by Kip2. Kip2 stabilizes microtubules by targeting Bik1 to the plus end and Kip2 levels are controlled during the cell cycle. As with Bik1, the targeting of dynein to the microtubule plus end requires Kip2. These findings reveal a central role for Kip2-dependent transport in the cell cycle control of microtubule dynamics and dynein-dependent motility.

Introduction

The dynamic behavior of microtubules (MTs) underlies many aspects of cellular and organismal morphogenesis. MTs are intrinsically polar polymers with a fast-growing plus end and a slow-growing minus end (Desai and Mitchison, 1997). In fungi and animals, the minus ends of MTs are usually at or adjacent to the microtubule organizing center and the plus ends are oriented peripherally. The plus ends of MTs form structural links to polarized membrane sites and kinetochores (Carvalho et al., 2003; Howard and Hyman, 2003).

A group of proteins called plus end tracking proteins or +TIPs specifically associate with the plus ends of MTs (Carvalho et al., 2003; Howard and Hyman, 2003). In live cell experiments, GFP-labeled +TIPs appear as comet- or dot-like structures that remain on the MT plus ends as they rocket through the cytoplasm (Perez et al., 1999). Plus end tracking was first described for the cytoplasmic linker protein CLIP-170 (Perez et al., 1999) and then observed for some other microtubule-associated proteins (MAPs) (Carvalho et al., 2003; Howard and Hyman, 2003). Many of the +TIPs that directly bind MTs also have important roles in controlling plus end dynamics (Han et al., 2001; Maiato et al., 2003; Rogers et al., 2002; Tirnauer et al., 1999, 2002). In addition to their role in promoting MT stability, CLIP-170-related proteins (CLIPs) may also guide the plus ends of MTs to polarized membrane sites (Brunner and Nurse, 2000; Komarova et al., 2002a, 2002b). CLIPs are also implicated in linking the MT plus ends to endocytic vesicles, to the leading edge of migrating cells and to kinetochores (Akhmanova et al., 2001; Dujardin et al., 1998; Fukata et al., 2002; Lin et al., 2001; Pierre et al., 1992; Coquelle et al., 2002; Tai et al., 2002; Gundersen, 2002).

Initial characterization of CLIP-170 suggested a simple treadmilling mechanism for plus end tracking. Using fluorescent speckle microscopy (FSM), Perez et al. demonstrated that CLIP-170 molecules bind to the ends of growing MTs, remain immobile after binding, and then rapidly dissociate behind the region of polymerization (Perez et al., 1999). Treadmilling behavior was subsequently observed for other MAPs such as EB1 (Tirnauer et al., 2002; Carvalho et al., 2003). This proposed treadmilling mechanism provided an elegant explanation for how the static MT binding of individual CLIP-170 molecules could be organized to produce a dynamic interaction between the population of CLIP-170 molecules and the growing plus end. Moreover, it was appealing to consider the possibility that treadmilling was a general mechanism for +TIPs because treadmilling could reflect an intrinsic link between plus end targeting and the mechanisms by which +TIPs control MT dynamics (Carvalho et al., 2003).

Recent studies suggest that treadmilling is not the only mechanism for plus end targeting. MT motors have also been implicated in the plus end localization of a number of +TIPs. Live cell imaging suggested that the adenomatous polyposis coli tumor suppressor protein (APC) undergoes ATP-dependent transport on MTs, and it was shown that APC binds to KIF3A-KIF3B kinesin motors (Jimbo et al., 2002; Mimori-Kiyosue et al., 2000). There is also indirect evidence for a motor-dependent mechanism for targeting budding yeast Kar9 to the plus end (Maekawa et al., 2003). Kar9 shares a small amount of homology with APC, and there are functional parallels between Kar9 and APC (Gundersen, 2002). In the fungus *Aspergillus*, the conventional kinesin KINA is required for the localization of dynein to the MT plus end (Zhang et al., 2003). Finally, in fission yeast, the CLIP-170 ortholog Tip1 requires the kinesin Tea2 for its normal pattern of localization (Browning et al., 2003). Live cell imaging demonstrates that Tea2 itself is a +TIP. In addition to motor-dependent mechanisms, there is a complex web of physical interactions among +TIPs and some +TIPs may hitchhike on other MAPs or motors more directly connected to the plus end (Carvalho et al., 2003; Howard and Hyman, 2003). The extent of these interactions highlights the importance of the MT plus end as a nodal point

*Correspondence: david_pellman@dfci.harvard.edu

for cytoskeletal integration, but it complicates studies of the mechanisms of plus end targeting.

Here we provide both a comprehensive characterization of the mechanism of plus end tracking by the budding yeast CLIP Bik1 and a dissection of the functional roles of Bik1 at the MT plus end. Our results demonstrate that Bik1 is transported to the plus and by the kinesin Kip2 (a homolog of Tea2). Kip2 was known to promote MT stability, but the mechanism was unknown (Cottingham and Hoyt, 1997; Huyett et al., 1998). We demonstrate that Kip2 regulates MTs by delivering Bik1 to the plus end, revealing a new mechanism by which kinesins may control MT dynamics. Kip2 protein levels vary during the cell cycle in a manner that correlates with the amount of plus end-bound Bik1 and with cell cycle-specific changes in MT dynamics. There are two major pathways for positioning the mitotic spindle in budding yeast, the preanaphase "Bim1/Kar9" pathway and the anaphase "dynein" pathway (Segal and Bloom, 2001). Explaining genetic data suggesting cooperation between Bik1, Kip2, and dynein (Miller et al., 1998; Sheeman et al., 2003; Tong et al., 2004), we found that Kip2 is necessary for the targeting of dynein to the plus end. This links the cell cycle control of Kip2 to the activation of dynein-dependent motility during anaphase.

Results

Bik1 Associates with the Plus Ends of Growing, Shrinking, and Pausing MTs

By single-color live cell microscopy we previously found that Bik1, like human CLIP-170, bound polymerizing MTs (Lin et al., 2001). To further characterize the mechanism of association of Bik1 with the MT plus end, we imaged a functional fusion between Bik1 and a 3YFP cassette (Bik1-3YFP) in cells in which MTs were also labeled with CFP-Tub1 (α-tubulin). As observed for Bik1-GFP constructs, Bik1-3YFP appeared as bright spots at the plus ends of the CFP-labeled MTs. However, two-color imaging revealed that Bik1 was at the plus end not only during MT growth, but also during depolymerization, a behavior that we term "backtracking" (Figure 1A and Supplemental Movie S1 [http://www.developmentalcell.com/cgi/content/full/6/6/815/DC1]). Fluorescence intensity measurements revealed that, although some fluctuations of the Bik1-3YFP signal were detected, there was no correlation between the intensity of the signal and periods of MT growth or shrinkage (Figure 1A). Consistent with the live cell imaging, in fixed cells Bik1-3YFP was detected at the plus ends of 97% of CFP-Tub1-labeled MTs ($n > 600$).

Bik1-3YFP bound the plus ends of both growing and shrinking MTs during all cell cycle stages. Bik1 also associated with both growing and shrinking MTs originating from both the mother- and the daughter-oriented SPBs (10–20 MTs were imaged for each class). Although observed during all cell cycle stages, the backtracking of Bik1 was less robust in unbudded G1 cells. In these cells, we frequently observed that during periods of MT depolymerization, the Bik1-3YFP signal intensity decreased (11/27 depolymerization events); however, it never completely disappeared (Figure 1B). Although the signal was less bright, Bik1 tagged with a single GFP (or YFP) behaved indistinguishably from Bik1-3GFP (or Bik1-3YFP [Supplemental Movies S2 and S3]).

The targeting of human CLIP-170 to the MT plus ends requires dynamic MTs (Diamantopoulos et al., 1999; Perez et al., 1999). We therefore characterized Bik1 localization in strains bearing a mutation in the β-tubulin gene (*TUB2*) that strikingly dampens MT dynamicity (Gupta et al., 2002). In *tub2-C354S* strains, MT polymerization and depolymerization rates are greatly reduced and the MTs spend most of their time in a paused state. However, in *tub2-C354S* cells, Bik1-3YFP was still targeted to the plus ends (in 99% of the cells; $n = 209$ [Figure 1C]). Thus, the plus end targeting of Bik1 does not require dynamic MTs.

The differences in behavior exhibited by Bik1 and CLIP-170 are not due to species-specific characteristics of their CAP-Gly MT binding domains. A chimera in which the Bik1 CAP-Gly domain was replaced by the corresponding domain from human CLIP-170 behaved like the native yeast protein (Supplemental Figure S1 and Movie S4). Thus, although Bik1, like CLIP-170, requires its CAP-Gly domain to bind MTs (Lin et al., 2001), the backtracking of Bik1 and its effective targeting to undynamic MTs contrasts with the reported properties of CLIP-170. These findings suggest mechanistic differences in how Bik1 and CLIP-170 are targeted to the MT plus end.

Three Cytoplasmic Pools of Bik1

Using fluorescence recovery after photobleaching (FRAP), we determined if the Bik1 at the plus end is dynamic. The bright spot of Bik1-3YFP at the plus end of the MTs was bleached with a laser that could be rapidly targeted by a galvanometer-driven mechanism (Figure 2A). The recovery of the Bik1-3YFP signal was imaged by rapid single focal plane time-lapse microscopy. Only MTs that remained in focus (monitored by CFP-Tub1 fluorescence) during the course of the experiment were analyzed ($n = 12$). We observed that Bik1-3YFP at the plus ends of MTs was dynamic with an average half-time of recovery of 19.2 s $\pm$12.9 (range 6.4 to 47.5 s) and an average maximal recovery of 59.6% $\pm$ 18.8 (range 27 to 86.8%). The turnover of the plus end-bound pool of Bik1 was confirmed by fluorescence loss in photobleaching (FLIP, data not shown). Of note, in 6/12 of the cells the recovery of the plus end occurred without any change in the length of the bleached MT (Figure 2B). Thus, our FRAP data support the idea that Bik1 is targeted to the plus end by a dynamic mechanism that is independent of MT dynamicity.

A significant pool of Bik1 is also present at or adjacent to the SPB. This signal includes Bik1 bound to the kinetochore (He et al., 2001; Lin et al., 2001), Bik1 bound to SPB proteins (Chen et al., 1998; Lin et al., 2001), and Bik1 bound to the plus ends of very short MTs. Because these pools of Bik1 cannot be resolved by light microscopy, they will hereafter be described as the "SPB-associated pool of Bik1." We again used FRAP to determine the turnover of Bik1 associated with the SPB. In most cells, there was no significant recovery of SPB-associated Bik1-3GFP after photobleaching, even when cells were imaged for up to several minutes ($n = 18$ observed, on average, for 521 s; range 285 to 864 s

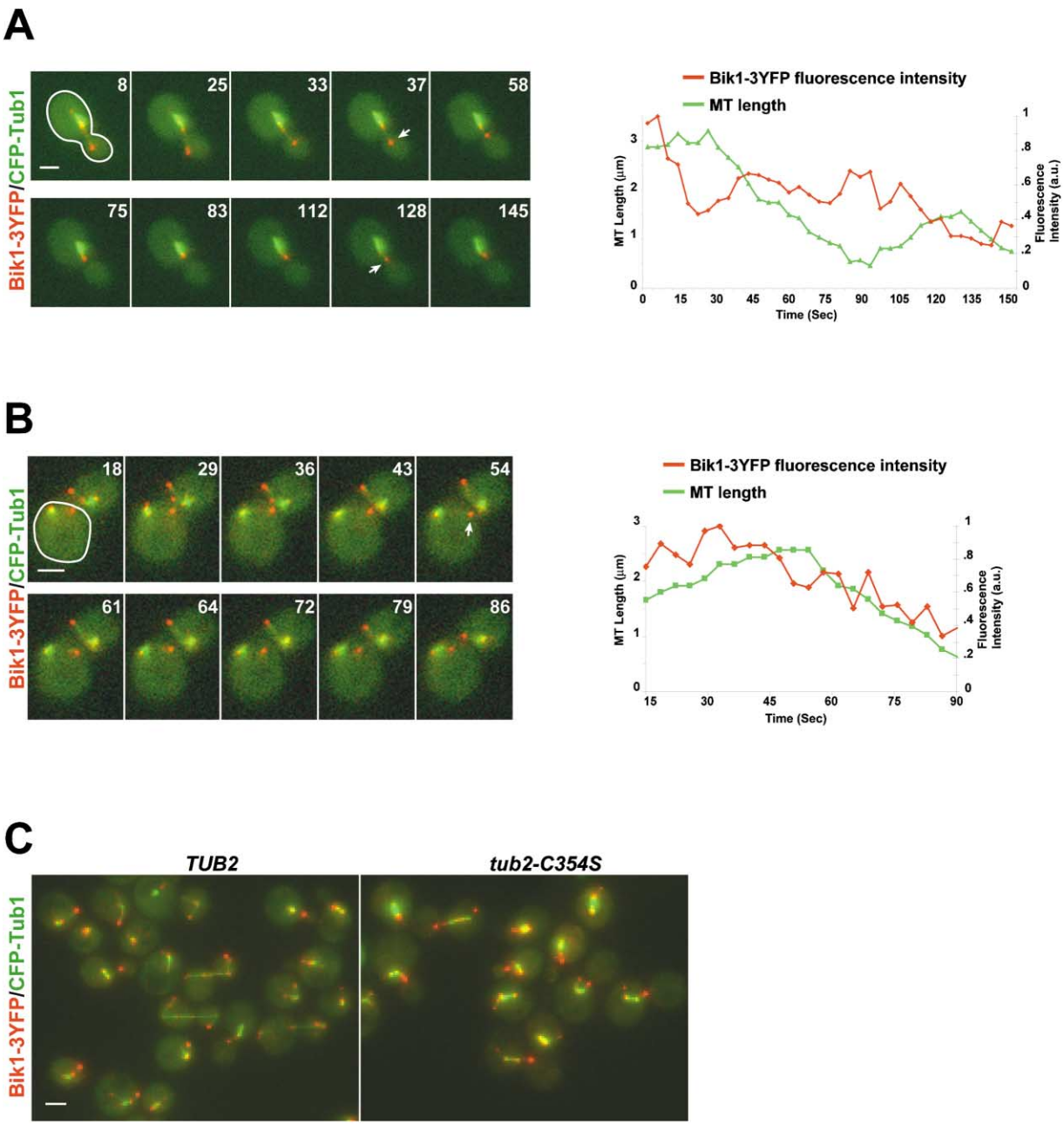

Figure 1. Bik1 Associates with the Plus Ends of Growing, Shrinking, and Paused MTs

Time-lapse images of preanaphase ([A], left) or G1 ([B], left) cells showing the association of a functional Bik1-3YFP fusion (red) with the plus ends of CFP-labeled MTs (green). Bik1-3YFP tracks the plus ends of both growing and shrinking MTs (arrows indicate MT plus ends prior to shrinkage). During preanaphase (A), the intensity of Bik1-3YFP signal at the MT plus ends does not correlate with periods of MT polymerization or depolymerization ([A], right). In G1 cells (B), Bik1-3YFP signal decreased (without totally disappearing) during MT shrinkage in 11/27 events, as shown for the outlined cell. Time is in seconds. (C) Plus end localization of Bik1-3YFP in merged stacks of fixed *tub2-C354S* cells. Scale bars equal 2 μm.

[Figure 2C]). Thus, the SPB-associated pool of Bik1 is clearly distinct from the pool that is visible at the plus ends of MTs.

The pool of Bik1 at the SPB might be the source of Bik1 loaded onto the MT plus end during the initiation of MTs. A SPB loading model was recently proposed for the +TIP Kar9 (Liakopoulos et al., 2003; Maekawa et al., 2003). Alternatively, the plus end-bound pool of Bik1 might be maintained by exchange with a third, soluble pool of Bik1. Although in most FRAP experiments Bik1 exhibited little turnover at the SPB, in a few cells, robust recovery of Bik1 was detected after bleaching of Bik1-3GFP at the SPB. In these cells, the fluorescence recovery was not correlated with the length of time after bleaching but rather with the abrupt movement of the recovered Bik1-3GFP signal away from

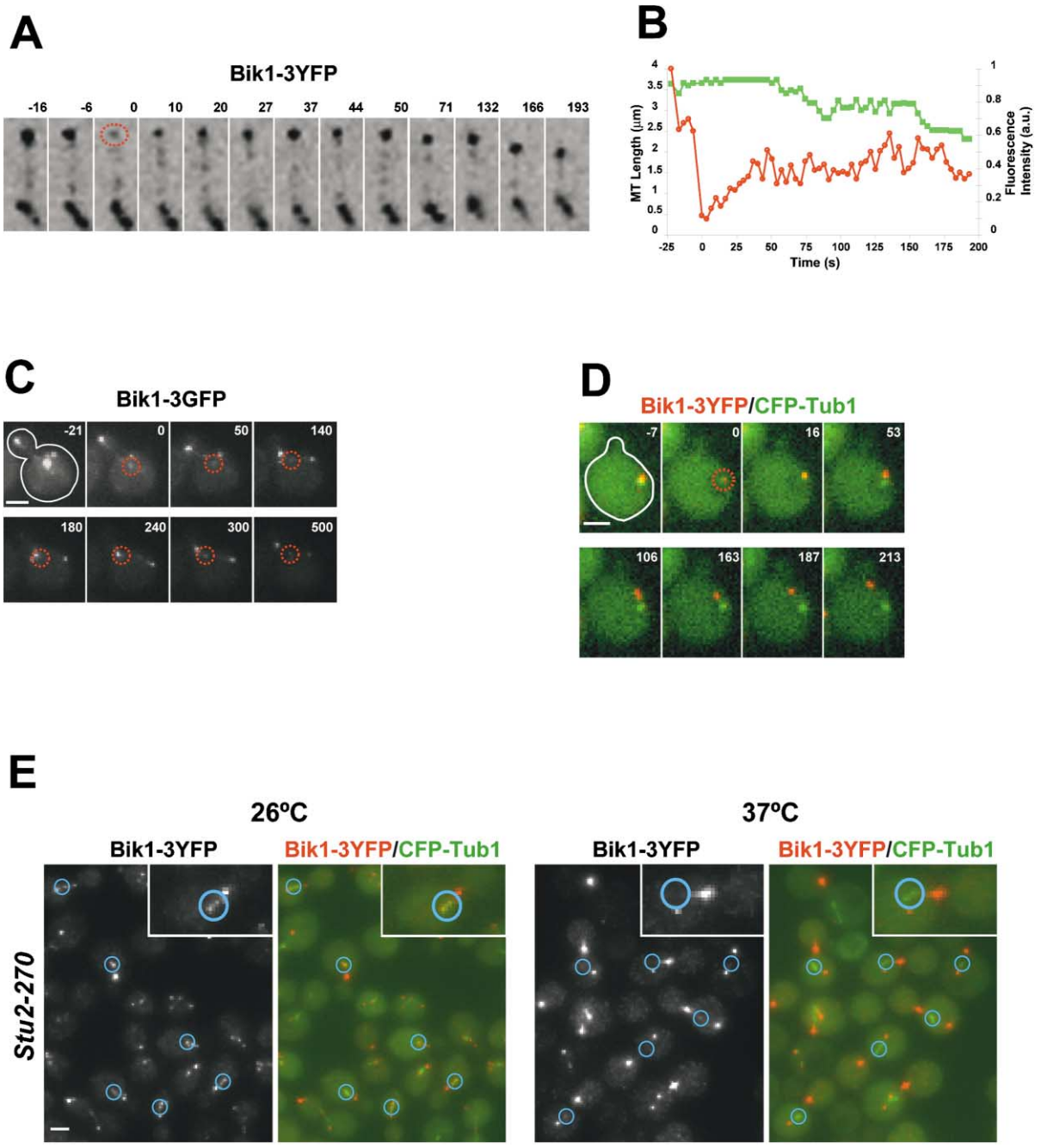

Figure 2. Distinct Cytoplasmic Pools of Bik1

(A) Bik1-3YFP at the plus ends of MTs is dynamic. 2D time-lapse image series showing a MT in which the plus end Bik1-3YFP signal was bleached (the zero time point is the first post-bleach image, red circle indicates bleached plus end signal).

(B) The recovery of Bik1-3YFP signal at the plus end (red line) occurs with no change in the MT length (green line).

(C) A population of Bik1-3GFP molecules is stably associated with the SPB/kinetochore. 2D projections of a 4D time-lapse image series from a cell in which Bik1-3GFP at the SPB was photobleached (circle indicates the bleached SPB).

(D) Bik1-3YFP can be recruited from the cytoplasm to the MT plus end during initiation of MT growth. In the indicated cell, the Bik1-3YFP (red) and CFP-Tub1 (green) signals were bleached. Note the rapid recovery of Bik1 signal. All of the Bik1-3YFP signal moves away from the SPB on the plus end of a growing MT. Because the photobleaching is not 100% complete, the SPB could be unambiguously tracked by contrast enhanced CFP-Tub1 signal. Time is in seconds.

(E) Bik1-3YFP is targeted to MT plus ends when the SPB-bound pool of Bik1 (SPBs encircled in blue) is eliminated by inactivation of *STU2* (note: loss of Bik1-3YFP is most obvious by comparison of black and white images). *stu2-270* and control cells were shifted to 37°C for 2 hr. Upon temperature shift, the Stu2-270 mutant protein is not associated with SPBs or MTs (data not shown). Insets show an enlarged representative cell. Scale bars equal 2 μm.

the SPB. This suggested that these recovery events corresponded to the initiation of a new MT (or elongation of a very short MT), with recruitment of Bik1 onto the plus end from a soluble pool. This was confirmed by two-color imaging experiments, which demonstrated that the recovery of Bik1 signal near the SPB was always preceded by the appearance of a MT (n = 9 [Figure 2D]). By monitoring the position of the recovered Bik1 signal over time, it was evident that this signal was invariably associated with the MT plus end. Thus, this experiment demonstrates the existence of a soluble pool of Bik1 that can exchange with the plus end.

Additional support for the idea that the SPB pool is not necessary for targeting Bik1 to the MT plus end came from studying strains where the MT binding protein Stu2 could be conditionally inactivated. Stu2 is the budding yeast homolog of the Dis1/TOG/XMAP215 family of MAPs (Kinoshita et al., 2002). At least a fraction of Bik1 and Stu2 molecules physically interact (Chen et al., 1998; Lin et al., 2001). Unlike Bik1, Stu2 is primarily concentrated at the SPB, with only a small amount of Stu2 detectable at the MT plus end (Kosco et al., 2001; Wang and Huffaker, 1997; data not shown). Strikingly, when a conditional allele of *stu2* is inactivated by a temperature shift (He et al., 2001), Bik1 signal is completely lost from the SPB but is still observed at the plus end (Figure 2E). Under the restrictive conditions, a fluorescent derivative of this mutant Stu2 protein (Stu2-270-3YFP) is also lost from the SPB (data not shown). This provides further support for the conclusion that Bik1 can be recruited onto the plus end from a soluble pool and that a SPB Bik1 pool is not essential for Bik1 plus end targeting.

Kip2 Is Required for the Efficient Targeting of Bik1 to the Plus End

In addition to the bright Bik1-3YFP signal at the plus ends of MTs and SPB/kinetochores, we also detected lower-intensity Bik1-3YFP speckles along the length of individual MTs (Figure 3). The ability to detect Bik1-3YFP speckles enabled us to use fluorescent speckle microscopy (FSM) to study the mechanism of Bik1-3YFP plus end targeting (Waterman-Storer and Salmon, 1997). By contrast with the reported behavior of CLIP-170 (Perez et al., 1999), Bik1-3YFP speckles along single MTs were highly dynamic (Figure 3A and Supplemental Movie S5). Kymographs demonstrated that Bik1-3YFP speckles move along the MT toward the plus end at a rate that exceeded that of MT polymerization (on average 6.6 μm/min; range 3.2 to 15.2 μm/min; 68 speckles from 32 MTs [Figure 3B]) (Carminati and Stearns, 1997; Shaw et al., 1997; Tirnauer et al., 1999). Measurements of the fluorescence intensity of the CFP-labeled MTs demonstrated that these speckles were along the body of the MT and did not represent Bik1-3YFP signal from the plus end of a short MT bundled together with a longer MT (Figure 3C). Although the bulk of the Bik1-3YFP speckles moved toward the plus end, we cannot exclude the possibility that a small percentage of speckles move toward the minus end. Thus, inconsistent with the treadmilling mechanism, Bik1-3YFP speckles are not stationary, but rather slide along the MT in a manner suggesting motor-dependent transport.

To determine the mechanism of Bik1 transport, we tested whether mutations in the MT motors that have been implicated in regulating cytoplasmic MT function affected Bik1 localization. A decrease of Bik1-3YFP on the population of MT plus ends was only observed for cells lacking the kinesin Kip2 (Average Fluorescence Intensity [Avg FI] = 88.5 arbitrary units [au] in *kip2*Δ versus Avg FI = 174.8 au in control cells; $n > 400$; $p < 0.001$ [Figure 4A]). Interestingly, this population of cells also had an increase of Bik1-3YFP at or near the SPB (Avg FI = 262.8 au in *kip2*Δ versus Avg FI = 107.8 au in control cells; $n > 100$; $p < 0.001$ [Figures 4A and 4B]). In a separate experiment, in which the minus and plus ends of individual MTs were directly compared, we observed that *kip2*Δ cells had on average an 8.5-fold decrease in the ratio of the fluorescence intensity at the plus end versus the SPB (0.35 in *kip2*Δ, n = 58; 3.03 in *wt*, n = 62; $p < 0.001$). The data were analyzed as box plots on a logarithmic scale, which normalizes the distribution of the ratios that are less than one to those greater than one (Figure 4C).

Although this result suggested that Kip2 might have a role in Bik1 plus end targeting, the very short MTs in *kip2*Δ cells limited the number of MTs in which we could reliably distinguish the plus end from the SPB. To circumvent this difficulty, we combined *kip2*Δ with *kar3-64*, a conditional allele of *KAR3*, which encodes a kinesin with MT depolymerase activity. Inactivation of Kar3 increases MT length while inactivation of Kar3 in combination with loss of Kip2 results in cells that have a normal average MT length (Cottingham et al., 1999; Huyett et al., 1998). By contrast with control *kar3-64* cells, Bik1-3YFP was markedly reduced from the plus ends of MTs in *kar3-64 kip2*Δ cells (Avg FI = 29.4 au in *kar3-64 kip2*Δ versus Avg FI =100.1 au in control cells; $n > 150$; $p < 0.001$ [Figure 4D]). Interestingly, this effect was dependent upon MT length: MTs 1–2 μm long exhibited some reduction in plus end-associated Bik1 whereas MTs longer than 2 μm exhibited a striking reduction in the amount of plus end associated Bik1 (Figure 4E). As observed in *kip2*Δ cells, the fluorescence intensity of Bik1-3YFP at the spindle pole body or very short MTs was also modestly increased in *kar3-64 kip2*Δ cells when compared to *kar3-64* controls (Avg FI = 109.8 au in *kar3-64 kip2*, n = 60; Avg FI = 97.7 au in *kar3-64*, n = 54). These data suggest that Kip2 might have a role in transporting Bik1 to or maintaining Bik1 at the MT plus end. Notably, this hypothesis could explain previous genetic data indicating overlapping function between Bik1 and Kip2 during dynein-dependent anaphase spindle movement (Miller et al., 1998; Sheeman et al., 2003; Tong et al., 2004).

Kip2 Localizes to MT Plus Ends

Previous studies have reported Kip2 localization either at the SPB or along the length of cytoplasmic MTs (Huyett et al., 1998; Miller et al., 1998). These previous studies either examined overexpressed Kip2 or did not colocalize Kip2 with MTs. We therefore reexamined Kip2 localization at endogenous levels in cells where tubulin could also be imaged (Figure 5A). A functional Kip2-3YFP fusion exhibited strong labeling of the MT plus end and, similar to Bik1, produced low-intensity speckles along MTs. By live cell imaging, the Kip2-3YFP speckles were

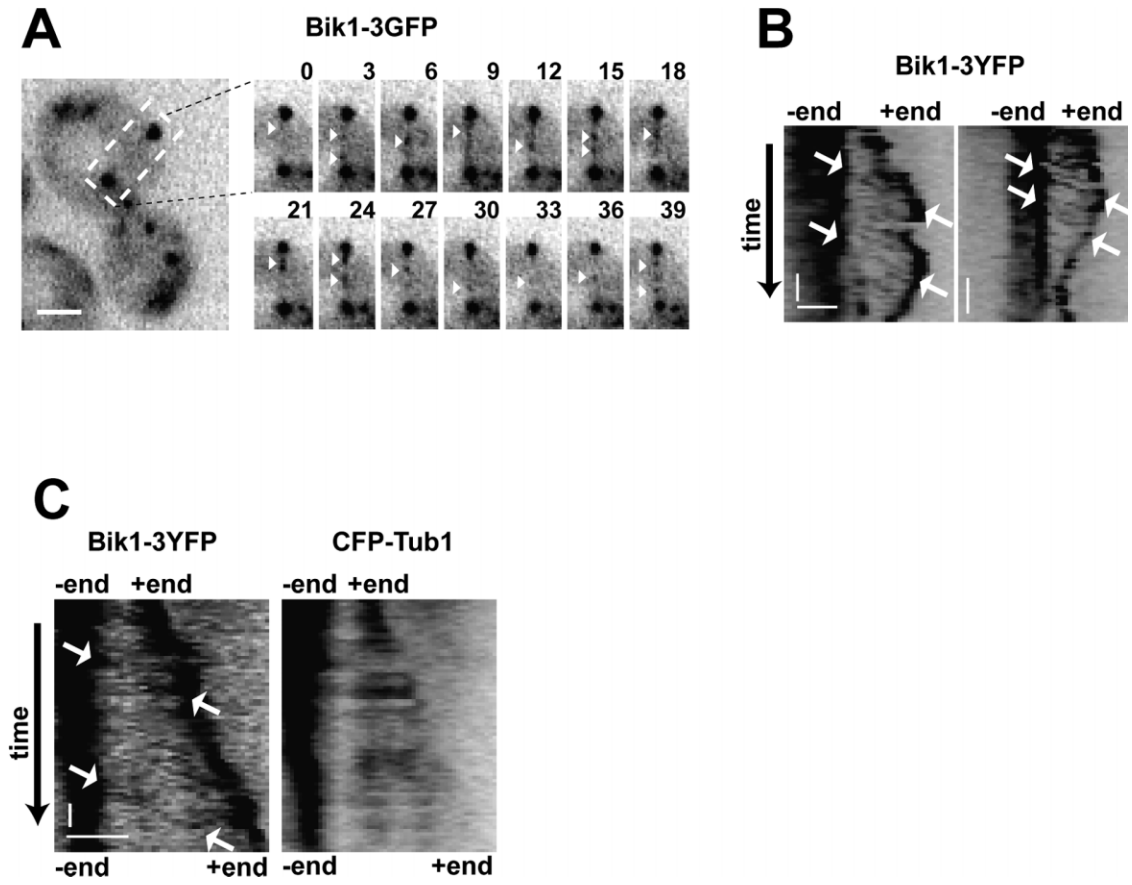

Figure 3. Bik1 Speckles Are Dynamic and Move toward the Plus Ends of MTs

(A) Time-lapse images showing that Bik1-3GFP speckles (white arrowheads) are dynamic. Time is in seconds. (B) Kymograph showing that Bik1-3YFP speckles (flanked by arrows) seem to move in a plus end-directed manner. (C) Kymographs of Bik1-3YFP- and CFP-Tub1-labeled MT. The CFP-Tub1 signal demonstrates that the diagonal streaks of Bik1-3YFP signal (flanked by arrows) do not represent the plus ends of short-growing MTs annealed to a longer MT. Vertical bar equals 40 s. Horizontal bar equals 2 μm.

highly dynamic and exhibited movement toward the MT plus ends (Figure 5B). However, unlike Bik1, Kip2-3YFP was not detected at the SPBs.

The fission yeast Kip2 homolog Tea2 also localizes to the plus ends of MTs (Browning et al., 2000). Interestingly, the localization of Tea2 to MTs was shown to require the EB1 homolog Mal3 (Browning et al., 2003). Based on this finding, it was proposed that Mal3 is required to load Tea2 when MTs are initiated (Browning et al., 2003). We therefore tested whether Bim1, the *S. cerevisiae* Mal3 homolog, is required for normal Kip2 localization. By contrast with fission yeast, Kip2-3YFP still labeled the plus ends in *bim1*Δ cells (Figure 5C). In fact, the amount of plus end-bound Kip2-3YFP was increased in *bim1*Δ cells (Avg FI = 144.2 au in *bim1*Δ versus Avg FI = 93.3 au in control cells; $n > 200$ for each strain; $p < 0.001$ [Figure 5D]). This finding demonstrates that EB1 orthologs do not have a general role in assembling Kip2-related kinesins onto MTs.

Bik1 and Kip2 Form a Complex and Comigrate along MTs

In addition to the localization pattern and the genetic data, other lines of evidence previously suggested that Bik1 and Kip2 might have common functions. First, the MT defects observed in *bik1*Δ and *kip2*Δ cells are similar (Berlin et al., 1990; Cottingham and Hoyt, 1997; Huyett et al., 1998; Miller et al., 1998; Sheeman et al., 2003). Second, a physical interaction between Bik1 and Kip2 was suggested by data from a large-scale two-hybrid screen for interactions between coiled-coil sequences (Newman et al., 2000). Indeed, we determined by coimmunoprecipitation of endogenously expressed proteins that Bik1 and Kip2 physically interact (Figure 5E).

Finally, we used dual-color FSM in a strain coexpressing Bik1-3CFP and Kip2-3YFP to determine if these proteins comigrated along individual MTs. First, single focal plane imaging demonstrated that Bik1-3CFP and Kip2-3YFP speckles colocalize along the length of individual MTs. Second, by time-lapse imaging we observed striking correspondence of the patterns of speckles formed by Bik1-3CFP and Kip2-3YFP (Figure 5F). In 6/7 kymographs, we observed that the diagonal streaks formed by Bik1-3CFP speckles had a very similar pattern to the streaks formed by Kip2-3YFP speckles (Figure 5G). Of note, the two patterns did not exactly overlap but were slightly offset in the time dimension, explainable by the expected delay introduced by the exposure times and

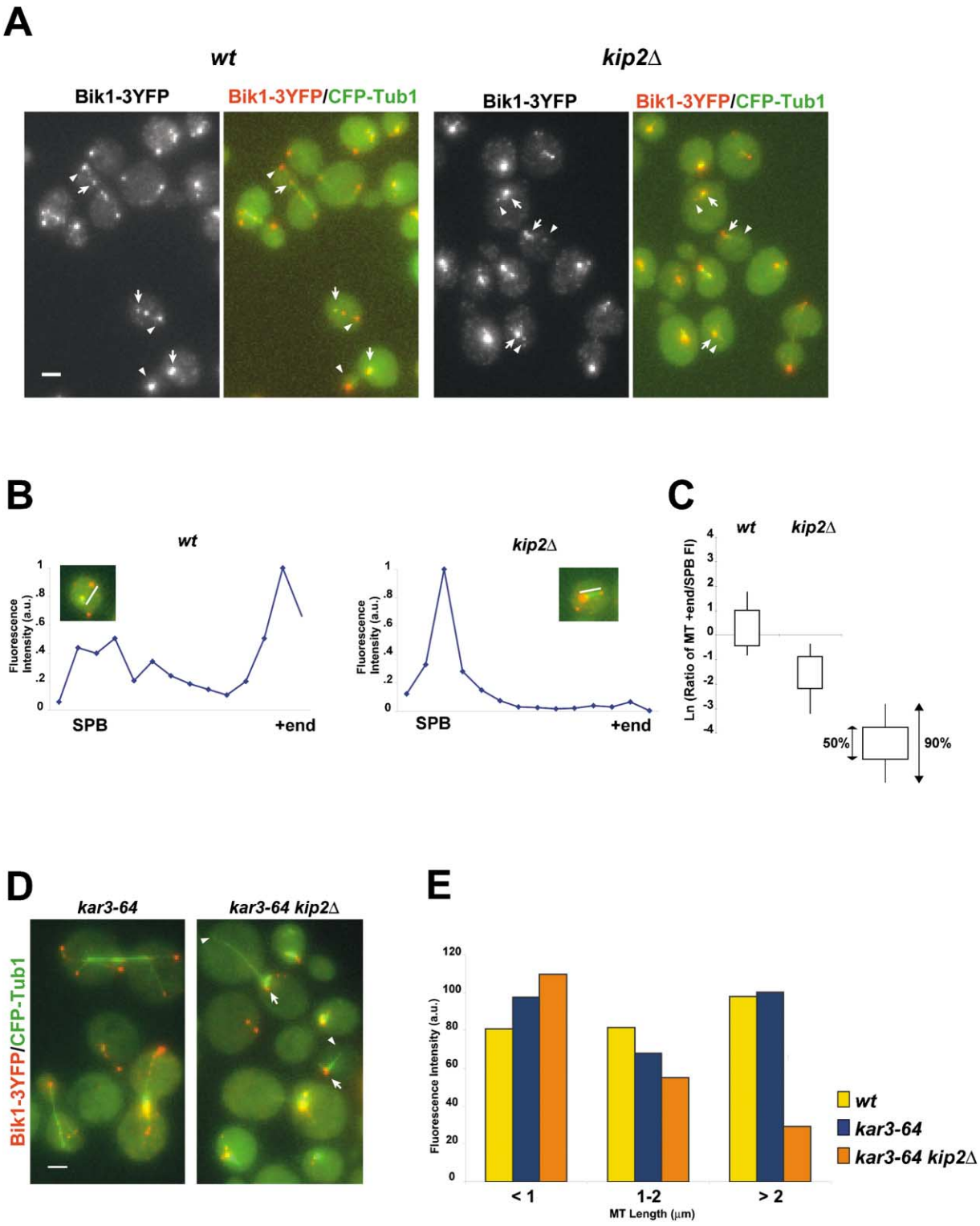

Figure 4. The Kinesin Kip2 Is Required for Efficient Targeting of Bik1 to MT Plus Ends

(A) Deletion of Kip2 results in a decrease of Bik1-3YFP (red) at the plus ends (arrowheads) of CFP-labeled MTs (green) with a concomitant increase of Bik1-3YFP labeling at or close to the SPBs (arrows).

(B) The fluorescence intensity of Bik1-3YFP along a representative MT (white line in the inset) showing the relative distribution of Bik1 between the plus and the minus MT end.

(C) Box plot showing the ratio between the Bik1-3YFP fluorescence intensity at the plus end and at the SPB for individual MTs in fixed *kip2*Δ and control cells. Note that the ratios are displayed on a logarithmic scale (see text).

(D) Although Bik1-3YFP is detected at the plus ends of MTs in *kar3-64* cells, Bik1-3YFP is virtually absent from the plus ends of the long MTs (arrowheads) in the *kar3-64 kip2*Δ cells. As observed in *kip2*Δ cells, in the *kar3-64 kip2*Δ cells Bik1-3YFP still concentrates at the SPB (arrows).

(E) Distribution of Bik1-3YFP fluorescence intensity at the plus ends of as function of the MT length. Scale bars equal 2 μm.

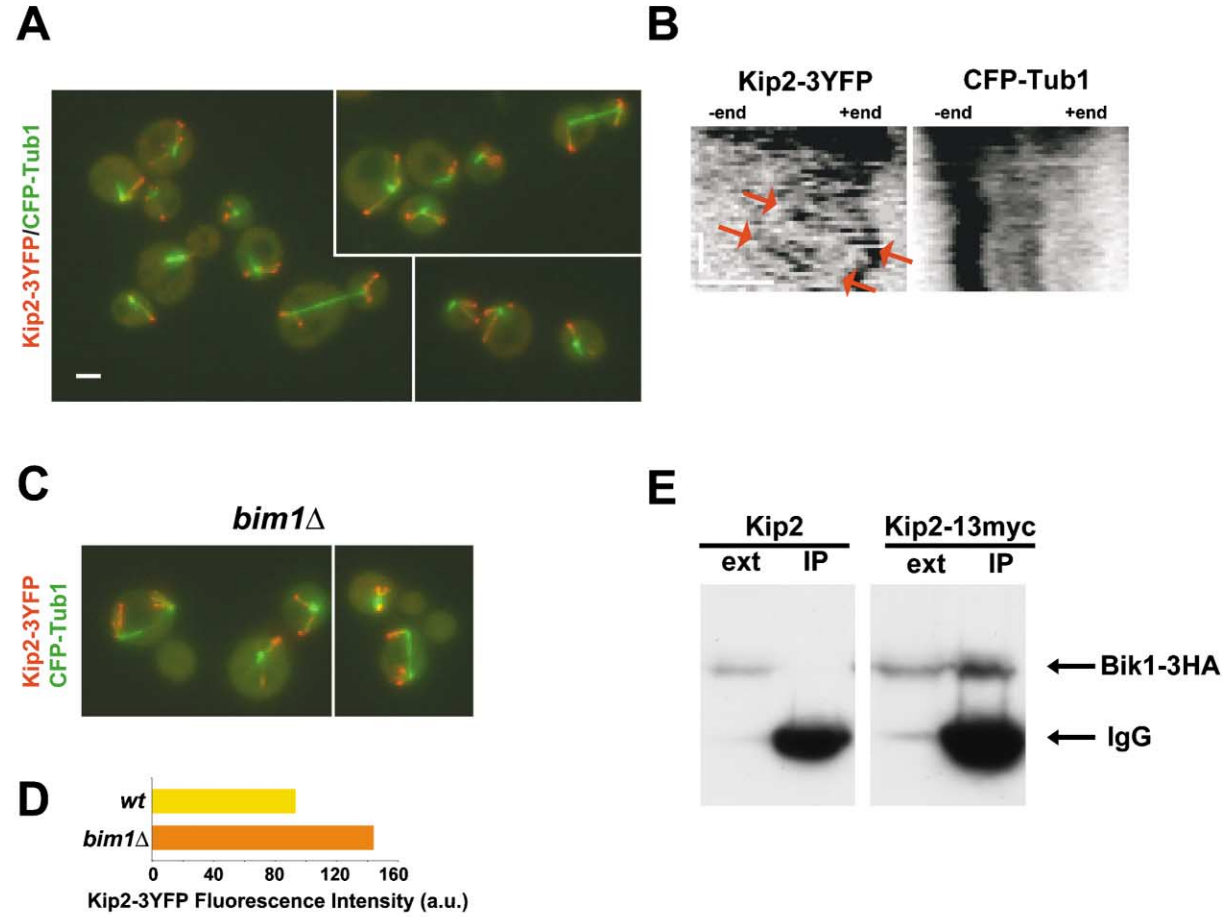

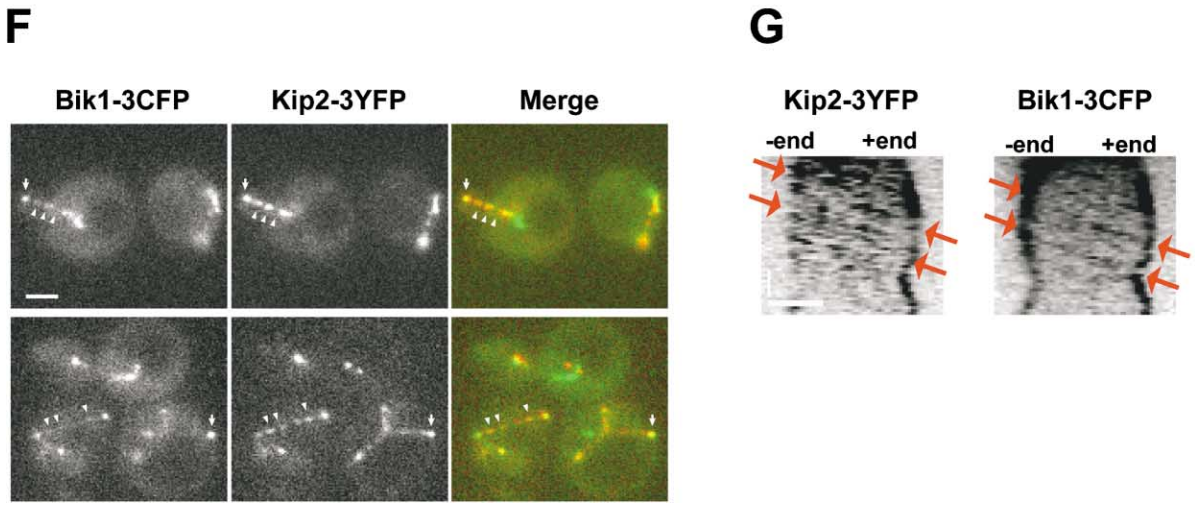

Figure 5. Kip2-3YFP Accumulates at the MT Plus End, Is in a Complex with Bik1, and Appears to Comigrate with Bik1 to the MT Plus Ends

(A) Kip2-3YFP (red) localizes to the plus ends of astral MTs, labeled with CFP-Tub1 (green). By contrast with Bik1, Kip2-3YFP is not detected at the SPBs. Images are 2D projections of 3D image stacks from cells expressing a functional Kip2-3YFP fusion expressed from the native promoter.

(B) Kymograph showing that Kip2-3YFP speckles (flanked by red arrows) move toward the plus ends of MTs.

(C) In cells lacking the +TIP Bim1, Kip2-3YFP still localizes to astral MTs.

(D) Fluorescence intensity measurements in populations of fixed cells reveal an increase of Kip2 on the astral MTs in *bim1*Δ cells (shown are measurements from MT plus ends).

(E) Endogenously expressed HA-tagged Bik1 coprecipitates with endogenously expressed myc-tagged Kip2. Lysates from cells expressing the indicated epitope-tagged proteins were immunoprecipitated with anti-myc mAb to precipitate Kip2 and blotted with anti-HA mAb to detect Bik1.

(F) Bik1-3CFP and Kip2-3YFP colocalize to the MT plus end (arrows) and partially overlap in discrete speckles along the MTs (arrowheads). Shown are single focal plane images of live cells coexpressing Kip2-3YFP (red in the merge) and Bik1-3CFP (green in the merge).

(G) Kymograph from a two-color time-lapse experiment illustrating the correspondence between Bik1-3CFP and Kip2-3YFP speckle movement (bottom panel). Bik1-3CFP or Kip2-3YFP speckles are flanked by arrows. Vertical bar equals 40 s. Horizontal bar equals 2 μm.

the time required to switch filter cubes. Thus, Kip2 binds Bik1 and likely transports it toward the MT plus end.

Kip2 Stabilizes MTs by Controlling the Amount of Bik1 at the Plus End

It has long been known that kinesins such as Kip2 are required for normal MT dynamics (Hildebrandt and Hoyt, 2000; Hunter and Wordeman, 2000; Sharp et al., 2000). However, except for the kinesins that have MT depolymerase activity, the mechanisms by which kinesin motors affect MT dynamics are not understood. Our findings raised the possibility that Kip2 affects MT dynamics by controlling the amount of plus end-associated Bik1. To test this hypothesis, we constructed a strain expressing GFP-Tub1 and bearing a plasmid that expresses Kip2 under the control of the inducible *GAL1* promoter. In wild-type cells, we observed that within 30–45 min after the induction of Kip2 expression, the MTs became remarkably elongated and stable, frequently curling around the cell cortex (Figure 6A). Strikingly, Kip2 overexpression failed to stabilize MTs in cells lacking Bik1, demonstrating that the MT stabilizing activity of Kip2 requires Bik1. This effect was not due to a decrease in the steady-state levels of Kip2 in *bik1*Δ cells (Supplemental Figure S2). Moreover, the Bik1 requirement was specific. Kip2 overexpression in cells lacking Bim1, another +TIP important for MT stability (Tirnauer et al., 1999), resulted in long and stable MTs similar to those produced by Kip2 overexpression in wild-type cells (Figure 6A). Finally, we observed that Kip2 overexpression had a dramatic effect on the intracellular distribution of Bik1-3YFP. Rapidly after induction of high levels of Kip2, all of the Bik1-3YFP signal associated with the MT plus ends (Figure 6B and Supplemental Figure S3). These results therefore suggest that Kip2 controls MT dynamics by a novel mechanism: the delivery of the +TIP Bik1 to the MT plus end.

Cell Cycle Regulation of Kip2 Levels Controls MT Stability and Dynein-Dependent Nuclear Movement

Microtubule dynamicity is regulated by the cell cycle machinery. In yeast, in contrast to higher eukaryotes, MTs are more dynamic during interphase compared to mitosis (Carminati and Stearns, 1997; Tirnauer et al., 1999; Adames and Cooper, 2000). Consistent with genome-wide expression analysis demonstrating that Kip2 mRNA is cell cycle regulated (Spellman et al., 1998), we found that Kip2 protein levels are cell cycle regulated, peaking during mitosis when MTs are more stable (Figure 7A and Supplemental Figure S4). The variation in the abundance of Kip2 is less dramatic than Clb2, in agreement with our fluorescence imaging in which lower levels of Kip2-3YFP were detected on cytoplasmic MTs in G1 cells. By fluorescence intensity measurements, the Bik1-3YFP signal at the plus ends of MTs increased approximately 2-fold during mitosis coincident with the increase in Kip2 protein levels (Avg FI = 64.94 au in G1 versus Avg FI = 122.20 au in mitotic cells; $n > 500$ for each cell cycle stage; $p < 0.001$). The increase in the plus end fluorescence of Bik1-3YFP was accompanied by a decrease of Bik1 at the SPBs (Figure 7B). This result further supports the conclusion that Kip2 stabilizes MTs by targeting Bik1 to the plus ends. Moreover, if backtracking requires constant replenishment of plus end-bound Bik1, the relatively low levels of Kip2 during G1 may explain our observation that backtracking of Bik1 is less robust during G1.

We recently found that Bik1 (Sheeman et al., 2003), in concert with Pac1/Lis1 (Sheeman et al., 2003; Lee et al., 2003), is required for the association of the dynein heavy chain with SPBs and MTs. Like Bik1, dynein is concentrated at the MT plus ends and may be delivered to the cell cortex by the plus ends of polymerizing MTs (Lee et al., 2003; Sheeman et al., 2003). Previous genetic crosses (Miller et al., 1998) and a recent genome-wide analysis (Tong et al., 2004) indicated that Kip2 is also required for dynein function. We therefore determined if Kip2 was required for the targeting of dynein to MT plus ends, as we observed for Bik1. By comparison with *kar3-64* cells, the association of Dyn1-3YFP with plus ends of longer MTs was lost in *kar3-64 kip2*Δ cells (Figures 7C and 7D). Thus, in addition to Bik1, Kip2 may target other dynein components to the MT plus end.

Discussion

CLIPs are a highly conserved family of MT regulators and were the first proteins shown to associate with the plus ends of MTs in vivo (Rickard and Kreis, 1990; Pierre et al., 1992). Defining how CLIPs are targeted to the plus end is important for understanding the control of MT dynamics and how other CLIP-dependent functions are regulated. In this study, we have comprehensively characterized the dynamic intracellular distribution of the budding yeast CLIP family member Bik1. Our results revealed a novel kinesin-dependent mechanism for targeting Bik1 to the MT plus end that suggest a new way by which kinesins can control MT dynamics. We defined different intracellular pools of Bik1 and elucidated how these pools contribute to plus end targeting. Finally, our findings have implications for both the cell cycle control of MT dynamics and the cell cycle control of dynein activity.

The Mechanisms for Targeting CLIPs to the Plus End of MTs

Studies on CLIP-170 suggested that it was targeted to the plus end by a mechanism that was intrinsically coupled to the dynamic behavior of MTs: treadmilling on polymerizing MTs (Diamantopoulos et al., 1999; Perez et al., 1999). Our characterization of the in vivo dynamics of Bik1 revealed striking contrasts with CLIP-170, suggesting that treadmilling is not the dominant plus end targeting mechanism for all CLIPs. Unlike CLIP-170, Bik1 can bind the plus ends of MTs independently of MT dynamics. This was evident from the fact that Bik1 binds both polymerizing as well as depolymerizing MTs, from the localization of Bik1 in *tub2-C354S* cells in which MT dynamics are strongly suppressed, and from our FRAP studies which showed rapid turnover of Bik1 on MT plus ends, irrespective of whether they were growing, shrinking, or paused. Moreover, FSM revealed the processive movement of YFP-labeled Bik1 speckles toward the plus end. Our imaging and biochemical data

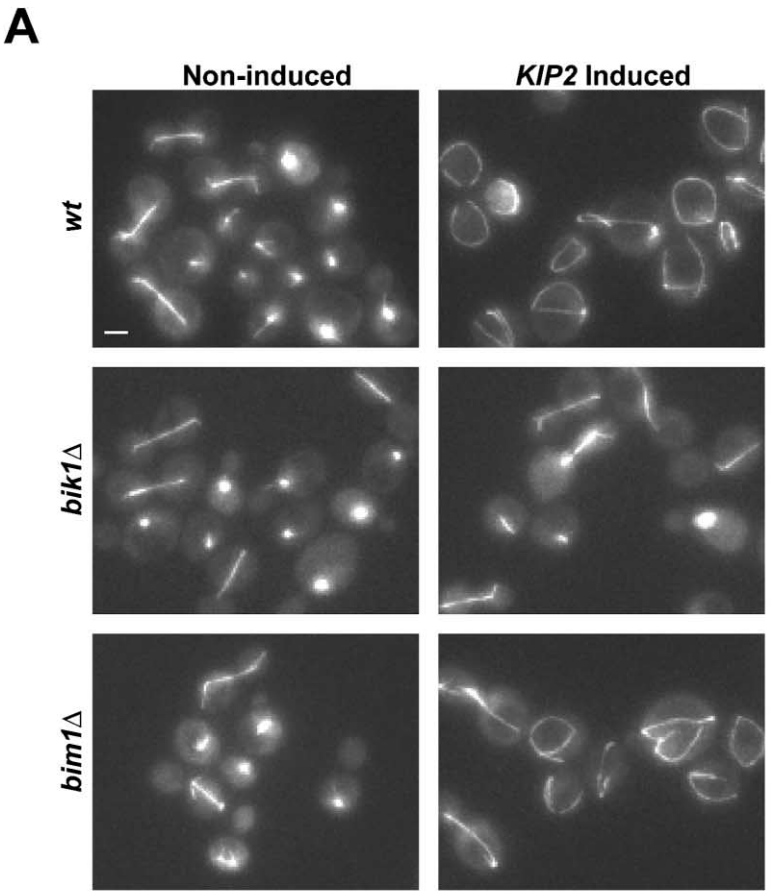

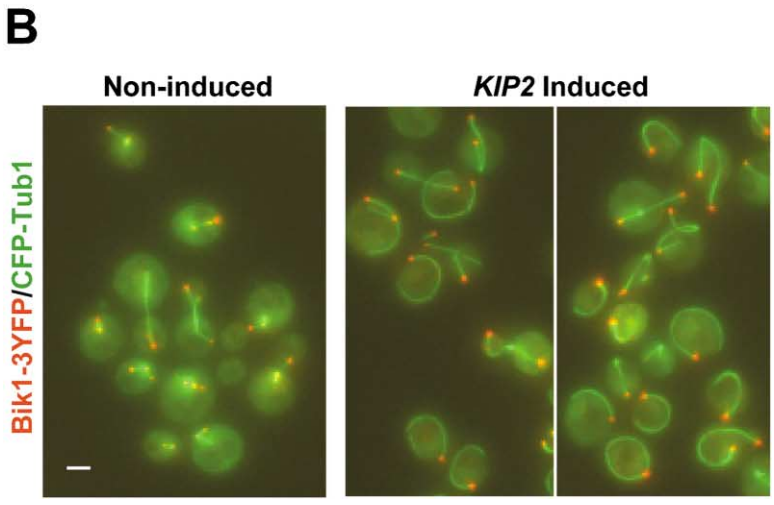

Figure 6. Kip2 Stabilizes MTs by Controlling the Delivery of Bik1 to the Plus End

(A) *KIP2* was overexpressed for 45 min from the *GAL1* promoter resulting in long and stable astral MTs in wild-type and *bim1*Δ cells but not in *bik1*Δ cells. Note that after long periods of Kip2 induction (2–3 hr) *BIK1*-independent aberrations in MTs were observed and *bik1*Δ does not abolish the lethality of *GAL-KIP2*. (B) Upon induction of *KIP2* overexpression, Bik1-3YFP (red) is highly concentrated at the plus ends of CFP-labeled MTs (green) and is depleted from the SPBs (see also Supplemental Figure S3). Bars equal 2 μm.

strongly support the idea that the kinesin Kip2 mediates the plus end-directed transport of Bik1.

Although Kip2 is clearly required for Bik1 to accumulate at MT plus ends, Bik1 appears to retain a diminished capacity to bind the plus ends of short MTs in *kip2*Δ mutant cells. Because the CAP-Gly domain of Bik1 is absolutely required for the plus end targeting of Bik1 (Lin et al., 2001), we favor the idea that the Kip2-independent MT binding represents an intrinsic affinity of the Bik1 CAP-Gly domain for the plus end. However, we cannot exclude the possibility that the residual plus end binding is mediated by other Bik1-interacting proteins such as Stu2 or Bim1 (Chen et al., 1998; Lin et al., 2001). For the control of astral MTs in mitotic cells, this residual binding of Bik1 to MTs in *kip2*Δ cells is unlikely to have great functional significance. *bik1*Δ and *kip2*Δ strains have similarly short astral MTs, a similar defect in dynein-dependent spindle movement, and, relative to the

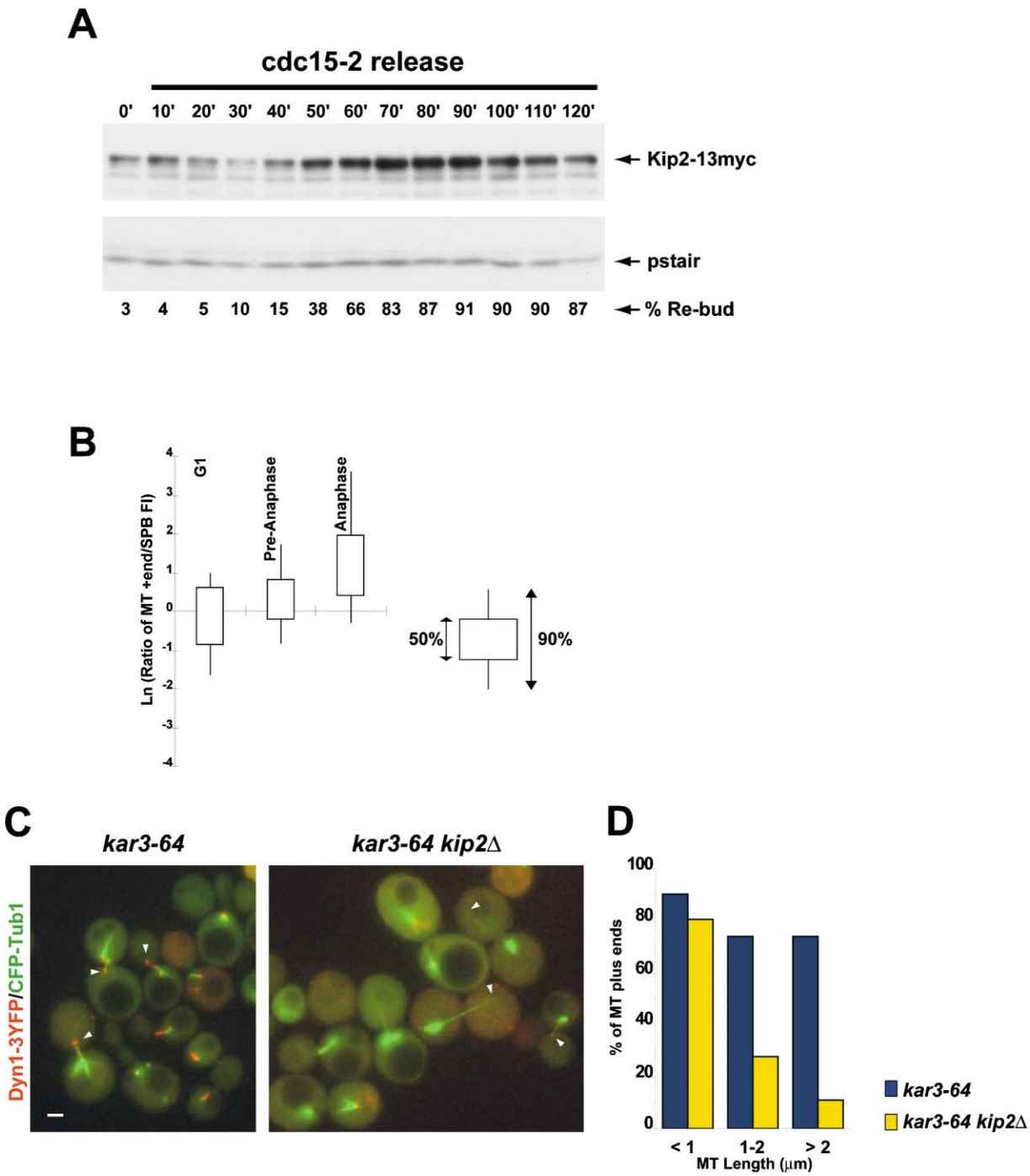

Figure 7. Cell Cycle Regulation of Kip2 Levels Controls MT Stability and Plus End Localization of Dynein

(A) *cdc15-2* cells were synchronized in telophase by incubation at 37°C for 2.5 hr. After release at 24°C, Kip2-13myc levels increase as cells progress through mitosis. Synchrony was confirmed scoring the percentage of cells that re-bud, and anti-PSTAIR was used for loading control.

(B) Box plot showing the ratio between the Bik1-3YFP fluorescence intensity at the plus end and at the SPB for individual MTs in fixed cells during different cell cycle stages. Note that the ratios are displayed on a logarithmic scale.

(C) At endogenous levels, Dyn-3YFP (red) is detected at the plus ends (arrowheads) of CFP-labeled MTs (green) in *kar3-64* cells but fails to localize in *kar3-64 kip2*Δ cells.

(D) Quantification of MT plus ends labeled with Dyn1-3YFP as a function of MT length. Bar equals 2 μm.

single mutants, *bik1*Δ *kip2*Δ strains do not exhibit additive defects in growth or nuclear migration (Berlin et al., 1990; Huyett et al., 1998; Miller et al., 1998; Sheeman et al., 2003; and our unpublished data).

Although Bik1 and Kip2 appear to function in concert to control astral MTs during mitosis, Bik1 has clearly distinct functions (Lin et al., 2001). Unlike Kip2, Bik1 localizes to kinetochores and spindle MTs (He et al.,

2001; Lin et al., 2001). Interestingly, the localization of Bik1 to the plus ends of interpolar MTs during anaphase does not require Kip2 (P.C. and D.P. unpublished data). Furthermore, Bik1 but not Kip2 is required for nuclear fusion after mating (Berlin et al., 1990; Miller et al., 1998). Thus, Bik1 may be a global MT stabilizer that is regionally regulated by other proteins, an emerging theme in the control of MT dynamics.

There are interesting similarities and contrasts between our studies of Bik1 and Kip2 and recent studies of their respective homologs in fission yeast, Tip1 and Tea2. Consistent with our results, cells lacking Tea2 (Kip2) have diminished Tip1 at the cell ends, presumably due to reduced delivery by MT plus ends (Browning et al., 2003). A similar defect in Tip1 localization was observed in cells expressing P loop (rigor) mutants of Tea2, demonstrating a requirement for ATP hydrolysis for normal Tea2 function (Browning et al., 2003). By live cell imaging, Tea2-GFP was exclusively observed at MT plus ends and not along the length of MTs. Because of this finding, it was suggested that Tea2 might have a novel ATP-dependent plus end binding activity rather than functioning as a conventional plus end-directed motor (Browning et al., 2003). By contrast, our FSM strongly suggests that Kip2 is a plus end-directed motor and that Kip2 transports Bik1 along MTs. Another difference between budding and fission yeast is the role of the EB1-related proteins in the targeting of the Bik1 and Kip2 homologs. The fission yeast EB1 homolog (Mal3) appears to be required for loading of both Tip1 and Tea2 onto MTs (Browning et al., 2003). However, we found that the amount of Kip2 bound to MTs was in fact increased in *bim1*Δ cells. Cells lacking *BIM1* were also observed to have enhanced plus end labeling of Bik1-3YFP and Dyn1-3YFP (P.C. and D.P., unpublished data). This increased MT-association of dynein components is likely to be functionally significant because premature dynein-dependent nuclear movements are observed in "Bim1/Kar9" pathway mutant cells (Lee et al., 1999; Yeh et al., 2000; Segal and Bloom, 2001). Thus, the previously suggested competition between the "Bim1/Kar9" and dynein pathways (Segal and Bloom, 2001) may occur by competitive binding of +TIPs to the MT plus end.

What is the significance of the apparent differences in how fungi and animal cells target CLIPs to the plus end? We consider the following possibilities. First, the systems may have evolved differently as an adaptation to differences in the dynamicity of their MTs. Yeast MTs are less dynamic than mammalian MTs, potentially constraining polymerization-coupled plus end-targeting mechanisms. However, we note that Bim1, like mammalian EB1, dissociates from depolymerizing MTs (Maddox et al., 2003; our unpublished data). Thus, although the Bim1 plus end-targeting mechanism needs to be better characterized, it is possible that yeast MTs might support a treadmilling-like direct binding mechanism. Second, it is possible that direct plus end binding and motor-dependent transport mechanisms are operative in both systems. The dynamics of CLIP-170 have only been studied on free cytoplasmic MTs and only in a limited number of cell types. It is possible that motor-dependent transport of CLIP-170 occurs but has not been detected because the appropriate classes of MTs, stimuli, or cell types have not yet been investigated.

Irrespective of the differences in plus end-targeting mechanisms between fungi and animal cells, CLIPs have remarkably similar functions at the MT plus ends. Animal and fungal CLIPs stabilize MTs as they extend from the centrosome to the cell cortex (Brunner and Nurse, 2000; Akhmanova et al., 2001; Komarova et al., 2002a). Animal and fungal CLIPs are also required to recruit dynein or dynein regulators to MTs (Coquelle et al., 2002; Tai et al., 2002; Sheeman et al., 2003; Dujardin et al., 2003). As observed in yeast (Han et al., 2001; Sheeman et al., 2003; Lee et al., 2003), a pool of dynein has recently been detected at the MT plus end in animal cells (Dujardin et al., 2003).

Kinesins, MAPs, and the Control of MT Behavior

Loss-of-function studies have implicated kinesins in the control of MT dynamics in many cell types (Hildebrandt and Hoyt, 2000; Hunter and Wordeman, 2000; Sharp et al., 2000). Although the underlying mechanism is apparent for the KinI-related kinesins that directly depolymerize MTs, the mechanism has been obscure for other kinesins (Desai et al., 1999; Hunter et al., 2003). Our results illustrate what may be an example of a general phenomenon: Kip2 controls the delivery of Bik1 to the plus end and thereby regulates plus end stability. This idea is supported by the fact that deletion of *BIK1* (but not *BIM1*) blocks MT stabilization induced by overexpression of Kip2. The adenomatous polyposis coli tumor suppressor (APC) appears to be transported to the plus end, potentially by the KIF3 kinesins (Dikovskaya et al., 2001; Jimbo et al., 2002; Mimori-Kiyosue et al., 2000). Although it is not known how this transport contributes to the known role of APC in regulating MT dynamics, it is appealing to speculate that this transport of APC shares common MT regulatory roles with the transport of Bik1 by Kip2.

The Cellular Pools of Bik1 and a Dynamic Initiation-Coupled Mechanism for Plus End Targeting

The development of a FRAP system that allowed rapid laser targeting on an epifluorescence microscope enabled us to characterize the intracellular pools of Bik1. We found that the SPB-associated Bik1 turned over very slowly while the plus end-bound pool of Bik1 was dynamic. Although we always saw Bik1 on the plus ends of cytoplasmic MTs that newly emerged from the SPB, the following evidence suggests that the SPB-bound pool of Bik1 is not required to load Bik1 onto the plus end: (1) When the SPB-associated Bik1 signal was eliminated by photobleaching, Bik1 could still be recruited onto the plus end from a soluble pool during MT initiation. (2) Bik1 was efficiently targeted to the plus end in *stu2-270* cells, where there is no detectable SPB-bound pool. Thus, although we cannot exclude the possibility that some of the SPB-associated Bik1 contributes to the plus end pool, these results demonstrate that a SPB-associated pool is not required for Bik1 plus end targeting. Moreover, these findings contrast with recent studies on the +TIP Kar9, where the SPB was suggested to function as a loading device for all of the plus end-associated Kar9 (Liakopoulos et al., 2003; Maekawa et al., 2003). During cell cycle progression, Bik1 diminishes

at the SPB but increases at the plus end. We speculate that for Bik1, the SPB may function like a "slow-release capsule," gradually increasing the amount of Bik1 in the soluble pool that is available for transport to the plus ends as cells progress through the cell cycle. Such a mechanism, in which the SPB titrates the availability of +TIPs, is in agreement with changes in the MT plus end dynamic observed in mutants for SPB components (Paluh et al., 2000; Usui et al., 2003; Vogel et al., 2001).

Kip2-Dependent Transport of Bik1 and the Cell Cycle Control of MT Dynamics and the Dynein Motor

Based on the findings presented in this paper, we propose the following provisional model for Bik1-dependent control of MT stability and spindle movement during cell division. In G1, Bik1 is enriched in a slowly exchangeable pool at the SPB, with a corresponding decrease in the amount of Bik1 available for transport to the plus end. A diminished level of soluble Bik1, together with lower levels of Kip2, results in less Bik1 at the MT plus end. The reduced amounts of plus end-bound Bik1 during G1 may prevent competition with Bim1 and Kar9, facilitating the initial Kar9-dependent step in spindle orientation and preventing premature activation of dynein (Segal and Bloom, 2001). Increased Kip2 levels during mitosis results in increased binding of Bik1-Kip2 complex along the length of cytoplasmic MTs, with a concomitant accumulation of dynein bound to the plus end. During mitosis, there is also loss of Bik1 from the SPB which might be due to cell cycle-specific regulation of proteins such as Stu2, or to competitive binding between Kip2 and Stu2 for Bik1. This mitosis-specific redistribution of Bik1 is likely to have important functional consequences. First, the enhanced delivery of Bik1 to the plus end during mitosis results in increased recruitment of dynein (Sheeman et al., 2003). Second, the increase in plus end-bound Bik1 promotes MT stability and facilitates the delivery of dynein to cortical sites, where it is then activated (Sheeman et al., 2003; Lee et al., 2003). The mitosis-specific increase in plus end-bound Bik1 may therefore make a significant contribution to the cell cycle-specific changes in cytoplasmic MT dynamics that are observed in budding yeast. We can envision a variety of other levels of control within this system, such as posttranslational regulation of Kip2. However, the results presented here provide a framework for understanding how +TIPs, MT motors, and cell cycle controls are integrated to distribute nuclei during cell division in budding yeast. The conserved functions of CLIPs and dynein suggest that our findings will also be relevant for the control of MT dynamics, spindle positioning, and asymmetric cell division in other eukaryotes.

Experimental Procedures

Yeast Genetics and Molecular Biology Techniques

Media and genetic techniques were as previously described (Rose et al., 1990). For a description of the strains and plasmids and characterization of the functionality of the epitope-tagged alleles, see Supplemental Experimental Procedures and Supplemental Table S1 (http://www.developmentalcell.com/cgi/content/full/6/6/815/DC1).

Fluorescence Imaging and Fluorescence Recovery after Photobleaching

Cells were observed in a fully automated Zeiss 200M inverted microscope (Carl Zeiss, Thornwood, NY) equipped with a MS-2000 stage (Applied Scientific Instrumentation, Eugene, OR), a Lambda LS 175 watt xenon light source (Sutter, Novato, CA), 63x and 100x 1.4NA Plan-Apochromat and 100x 1.45 Plan-Fluar objectives, and a 5 position filter turret. Images were acquired using a CoolSnap HQ camera (Roper Scientific, Tucson, AZ). The microscope, camera, and shutters (Uniblitz, Rochester, NY) were controlled by SlideBook software (Intelligent Imaging Innovations, Inc., Denver, CO).

All imaging was performed in log phase cells cultured in SC media supplemented with adenine. Strains bearing temperature-sensitive alleles were grown overnight at 26°C and shifted to 37°C prior to fixation and microscopic examination. All other strains were grown at 30°C. Cells were fixed in formaldehyde for 10 min and washed twice in phosphate-buffered saline solution before microscopic observation. For time-lapse live cell microscopy, 2–2.5 μl of the culture was spotted onto a glass slide and immediately imaged at room temperature (approximately 24°C).

Fluorescence recovery after photobleaching (FRAP) was performed using the Micropoint wavelength-tunable laser system (Photonics Instruments, St. Charles, IL) attached to the epi-illuminator port of the microscope. This system utilizes a nitrogen pulse laser (VSL-337ND-S; Laser Science, Franklin, MA) coupled to the microscope by a fiber optic cable. Incoherent light was synchronized and amplified using a coumarin blue chemical chamber, which emits at a wavelength of 440 nanometers. Simultaneous photobleaching and fluorescence illumination was achieved using a beamsplitter (95% Illumination/5% Laser) to direct both the fluorescence light and the laser beam into the fluorescence light train of the microscope. The XY targeting of the laser is controlled by two computer driven galvanometer-based steering lenses.

Analysis of Microscopy Data

All image manipulations and fluorescence intensity measurements were performed using SlideBook software and exported to and analyzed in Microsoft Excel. Measurements of FRAP were made as previously described (Salmon and Wadsworth, 1986; Schuyler et al., 2003). The fluorescence intensity of a 3 X 3 pixel square (0.36 μm^2) was measured at each time point for the bleached area. The intensity measurements were corrected for both background fluorescence (using background values of the bleached cell) and loss of fluorescence that occurred during imaging (using average background fluorescence of 5–10 unbleached neighbor cells).

Biochemical Methods

Immunoprecipitation and Western blotting were performed as described (Lee et al., 2000).

Acknowledgments

We dedicate this work to the memory of Brina Sheeman-Shackelford. We thank A. Amon, K. Bloom, X. He, M. Rose, P. Silver, P. Sorger, and A. Straight for strains and/or reagents, M. Berezuk for preliminary experiments, Y. Barral, D. Brunner, F. Chang, and members of the Pellman lab for discussions, and I. Sagot, C. Sunkel, J.S. Tirnauer, and S. Yoshida for critically reading the manuscript. P.C. thanks C. Sunkel for advice and support during the course of this project. P.C. is a PhD student of the GABBA Graduate Program of Oporto University (Portugal) and was supported by a fellowship from FCT (Praxis XXI/BD/20041/99). D.P. was supported by NIH RO1 GM61345-04 and a Scholar Award from the Leukemia and Lymphoma Society of America.

Received: February 11, 2004
Revised: April 6, 2004
Accepted: April 6, 2004
Published: June 7, 2004

References

Adames, N.R., and Cooper, J.A. (2000). Microtubule interactions with the cell cortex causing nuclear movements in *Saccharomyces cerevisiae*. J. Cell Biol. *149*, 863–874.

Akhmanova, A., Hoogenraad, C.C., Drabek, K., Stepanova, T., Dortland, B., Verkerk, T., Vermeulen, W., Burgering, B.M., De Zeeuw, C.I., Grosveld, F., and Galjart, N. (2001). Clasps are CLIP-115 and -170 associating proteins involved in the regional regulation of microtubule dynamics in motile fibroblasts. Cell *104*, 923–935.

Berlin, V., Styles, C.A., and Fink, G.R. (1990). BIK1, a protein required for microtubule function during mating and mitosis in *Saccharomyces cerevisiae*, colocalizes with tubulin. J. Cell Biol. *111*, 2573–2586.

Browning, H., Hayles, J., Mata, J., Aveline, L., Nurse, P., and Mcintosh, J.R. (2000). Tea2p is a kinesin-like protein required to generate polarized growth in fission yeast. J. Cell Biol. *151*, 15–28.

Browning, H., Hackney, D.D., and Nurse, P. (2003). Targeted movement of cell end factors in fission yeast. Nat. Cell Biol. *5*, 812–818.

Brunner, D., and Nurse, P. (2000). CLIP170-like tip1p spatially organizes microtubular dynamics in fission yeast. Cell *102*, 695–704.

Carminati, J.L., and Stearns, T. (1997). Microtubules orient the mitotic spindle in yeast through dynein-dependent interactions with the cell cortex. J. Cell Biol. *138*, 629–641.

Carvalho, P., Tirnauer, J.S., and Pellman, D. (2003). Surfing on microtubule ends. Trends Cell Biol. *13*, 229–237.

Chen, X.P., Yin, H., and Huffaker, T.C. (1998). The yeast spindle pole body component Spc72p interacts with Stu2p and is required for proper microtubule assembly. J. Cell Biol. *141*, 1169–1179.

Coquelle, F.M., Caspi, M., Cordelieres, F.P., Dompierre, J.P., Dujardin, D.L., Koifman, C., Martin, P., Hoogenraad, C.C., Akhmanova, A., Galjart, N., et al. (2002). LIS1, CLIP-170's key to the dynein/dynactin pathway. Mol. Cell. Biol. *22*, 3089–3102.

Cottingham, F.R., and Hoyt, M.A. (1997). Mitotic spindle positioning in *Saccharomyces cerevisiae* is accomplished by antagonistically acting microtubule motor proteins. J. Cell Biol. *138*, 1041–1053.

Cottingham, F.R., Gheber, L., Miller, D.L., and Hoyt, M.A. (1999). Novel roles for *Saccharomyces cerevisiae* mitotic spindle motors. J. Cell Biol. *147*, 335–350.

Desai, A., and Mitchison, T.J. (1997). Microtubule polymerization dynamics. Annu. Rev. Cell Dev. Biol. *13*, 83–117.

Desai, A., Verma, S., Mitchison, T.J., and Walczak, C.E. (1999). Kin I kinesins are microtubule-destabilizing enzymes. Cell *96*, 69–78.

Diamantopoulos, G.S., Perez, F., Goodson, H.V., Batelier, G., Melki, R., Kreis, T.E., and Rickard, J.E. (1999). Dynamic localization of CLIP-170 to microtubule plus ends is coupled to microtubule assembly. J. Cell Biol. *144*, 99–112.

Dikovskaya, D., Zumbrunn, J., Penman, G.A., and Nathke, I.S. (2001). The adenomatous polyposis coli protein: in the limelight out at the edge. Trends Cell Biol. *11*, 378–384.

Dujardin, D., Wacker, U.I., Moreau, A., Schroer, T.A., Rickard, J.E., and De Mey, J.R. (1998). Evidence for a role of CLIP-170 in the establishment of metaphase chromosome alignment. J. Cell Biol. *141*, 849–862.

Dujardin, D.L., Barnhart, L.E., Stehman, S.A., Gomes, E.R., Gundersen, G.G., and Vallee, R.B. (2003). A role for cytoplasmic dynein and LIS1 in directed cell movement. J. Cell Biol. *163*, 1205–1211.

Fukata, M., Watanabe, T., Noritake, J., Nakagawa, M., Yamaga, M., Kuroda, S., Matsuura, Y., Iwamatsu, A., Perez, F., and Kaibuchi, K. (2002). Rac1 and Cdc42 capture microtubules through IQGAP1 and CLIP-170. Cell *109*, 873–885.

Gundersen, G.G. (2002). Evolutionary conservation of microtubule-capture mechanisms. Nat. Rev. Mol. Cell Biol. *3*, 296–304.

Gupta, M.L., Jr., Bode, C.J., Thrower, D.A., Pearson, C.G., Suprenant, K.A., Bloom, K.S., and Himes, R.H. (2002). β-Tubulin C354 mutations that severely decrease microtubule dynamics do not prevent nuclear migration in yeast. Mol. Biol. Cell *13*, 2919–2932.

Han, G., Liu, B., Zhang, J., Zuo, W., Morris, N.R., and Xiang, X. (2001). The *Aspergillus* cytoplasmic dynein heavy chain and NUDF localize to microtubule ends and affect microtubule dynamics. Curr. Biol. *11*, 719–724.

He, X., Rines, D.R., Espelin, C.W., and Sorger, P.K. (2001). Molecular analysis of kinetochore-microtubule attachment in budding yeast. Cell *106*, 195–206.

Hildebrandt, E.R., and Hoyt, M.A. (2000). Mitotic motors in *Saccharomyces cerevisiae*. Biochim. Biophys. Acta *1496*, 99–116.

Howard, J., and Hyman, A.A. (2003). Dynamics and mechanics of the microtubule plus end. Nature *422*, 753–758.

Hunter, A.W., and Wordeman, L. (2000). How motor proteins influence microtubule polymerization dynamics. J. Cell Sci. *113*, 4379–4389.

Hunter, A.W., Caplow, M., Coy, D.L., Hancock, W.O., Diez, S., Wordeman, L., and Howard, J. (2003). The kinesin-related protein MCAK is a microtubule depolymerase that forms an ATP-hydrolyzing complex at microtubule ends. Mol. Cell *11*, 445–457.

Huyett, A., Kahana, J., Silver, P., Zeng, X., and Saunders, W.S. (1998). The Kar3p and Kip2p motors function antagonistically at the spindle poles to influence cytoplasmic microtubule numbers. J. Cell Sci. *111*, 295–301.

Jimbo, T., Kawasaki, Y., Koyama, R., Sato, R., Takada, S., Haraguchi, K., and Akiyama, T. (2002). Identification of a link between the tumour suppressor APC and the kinesin superfamily. Nat. Cell Biol. *4*, 323–327.

Kinoshita, K., Habermann, B., and Hyman, A.A. (2002). XMAP215: a key component of the dynamic microtubule cytoskeleton. Trends Cell Biol. *12*, 267–273.

Komarova, Y.A., Akhmanova, A.S., Kojima, S., Galjart, N., and Borisy, G.G. (2002a). Cytoplasmic linker proteins promote microtubule rescue in vivo. J. Cell Biol. *159*, 589–599.

Komarova, Y.A., Vorobjev, I.A., and Borisy, G.G. (2002b). Life cycle of MTs: persistent growth in the cell interior, asymmetric transition frequencies and effects of the cell boundary. J. Cell Sci. *115*, 3527–3539.

Kosco, K.A., Pearson, C.G., Maddox, P.S., Wang, P.J., Adams, I.R., Salmon, E.D., Bloom, K., and Huffaker, T.C. (2001). Control of microtubule dynamics by Stu2p is essential for spindle orientation and metaphase chromosome alignment in yeast. Mol. Biol. Cell *12*, 2870–2880.

Lee, L., Klee, S.K., Evangelista, M., Boone, C., and Pellman, D. (1999). Control of mitotic spindle position by the *Saccharomyces cerevisiae* formin Bni1p. J. Cell Biol. *144*, 947–961.

Lee, L., Tirnauer, J.S., Li, J., Schuyler, S.C., Liu, J.Y., and Pellman, D. (2000). Positioning of the mitotic spindle by a cortical-microtubule capture mechanism. Science *287*, 2260–2262.

Lee, W.L., Oberle, J.R., and Cooper, J.A. (2003). The role of the lissencephaly protein Pac1 during nuclear migration in budding yeast. J. Cell Biol. *160*, 355–364.

Liakopoulos, D., Kusch, J., Grava, S., Vogel, J., and Barral, Y. (2003). Asymmetric loading of Kar9 onto spindle poles and microtubules ensures proper spindle alignment. Cell *112*, 561–574.

Lin, H., De Carvalho, P., Kho, D., Tai, C.Y., Pierre, P., Fink, G.R., and Pellman, D. (2001). Polyploids require Bik1 for kinetochore-microtubule attachment. J. Cell Biol. *155*, 1173–1184.

Maddox, P.S., Stemple, J.K., Satterwhite, L., Salmon, E.D., and Bloom, K. (2003). The minus end-directed motor Kar3 is required for coupling dynamic microtubule plus ends to the cortical shmoo tip in budding yeast. Curr. Biol. *13*, 1423–1428.

Maekawa, H., Usui, T., Knop, M., and Schiebel, E. (2003). Yeast Cdk1 translocates to the plus end of cytoplasmic microtubules to regulate bud cortex interactions. EMBO J. *22*, 438–449.

Maiato, H., Fairley, E.A., Rieder, C.L., Swedlow, J.R., Sunkel, C.E., and Earnshaw, W.C. (2003). Human CLASP1 is an outer kinetochore component that regulates spindle microtubule dynamics. Cell *113*, 891–904.

Miller, R.K., Heller, K.K., Frisen, L., Wallack, D.L., Loayza, D., Gammie, A.E., and Rose, M.D. (1998). The kinesin-related proteins, Kip2p and Kip3p, function differently in nuclear migration in yeast. Mol. Biol. Cell *9*, 2051–2068.

Mimori-Kiyosue, Y., Shiina, N., and Tsukita, S. (2000). Adenomatous polyposis coli (APC) protein moves along microtubules and concentrates at their growing ends in epithelial cells. J. Cell Biol. *148*, 505–518.

Newman, J.R., Wolf, E., and Kim, P.S. (2000). A computationally

directed screen identifying interacting coiled coils from *Saccharomyces cerevisiae*. Proc. Natl. Acad. Sci. USA *97*, 13203–13208.

Paluh, J.L., Nogales, E., Oakley, B.R., McDonald, K., Pidoux, A.L., and Cande, W.Z. (2000). A mutation in gamma-tubulin alters microtubule dynamics and organization and is synthetically lethal with the kinesin-like protein pkl1p. Mol. Biol. Cell *11*, 1225–1239.

Perez, F., Diamantopoulos, G.S., Stalder, R., and Kreis, T.E. (1999). CLIP-170 highlights growing microtubule ends in vivo. Cell *96*, 517–527.

Pierre, P., Scheel, J., Rickard, J.E., and Kreis, T.E. (1992). CLIP-170 links endocytic vesicles to microtubules. Cell *70*, 887–900.

Rickard, J.E., and Kreis, T.E. (1990). Identification of a novel nucleotide-sensitive microtubule-binding protein in HeLa cells. J. Cell Biol. *110*, 1623–1633.

Rogers, S.L., Rogers, G.C., Sharp, D.J., and Vale, R.D. (2002). *Drosophila* EB1 is important for proper assembly, dynamics, and positioning of the mitotic spindle. J. Cell Biol. *158*, 873–884.

Rose, M.D., Winston, F., and Hieter, P. (1990). Methods in Yeast Genetics (Cold Spring Harbor, NY: Cold Spring Harbor Laboratory Press).

Salmon, E.D., and Wadsworth, P. (1986). In Applications of Fluorescence in Biomedical Sciences, D.L. Taylor, F. Lanni, R.F. Murphy, and R.R. Birge, eds. (New York: Alan R. Liss), pp. 377–403.

Schuyler, S.C., Liu, J.Y., and Pellman, D. (2003). The molecular function of Ase1p: evidence for a MAP-dependent midzone-specific spindle matrix. Microtubule-associated proteins. J. Cell Biol. *160*, 517–528.

Segal, M., and Bloom, K. (2001). Control of spindle polarity and orientation in *Saccharomyces cerevisiae*. Trends Cell Biol. *11*, 160–166.

Sharp, D.J., Rogers, G.C., and Scholey, J.M. (2000). Microtubule motors in mitosis. Nature *407*, 41–47.

Shaw, S.L., Yeh, E., Maddox, P., Salmon, E.D., and Bloom, K. (1997). Astral microtubule dynamics in yeast: a microtubule-based searching mechanism for spindle orientation and nuclear migration into the bud. J. Cell Biol. *139*, 985–994.

Sheeman, B., Carvalho, P., Sagot, I., Geiser, J., Kho, D., Hoyt, M.A., and Pellman, D. (2003). Determinants of *S. cerevisiae* dynein localization and activation: implications for the mechanism of spindle positioning. Curr. Biol. *13*, 364–372.

Spellman, P.T., Sherlock, G., Zhang, M.Q., Iyer, V.R., Anders, K., Eisen, M.B., Brown, P.O., Botstein, D., and Futcher, B. (1998). Comprehensive identification of cell cycle-regulated genes of the yeast *Saccharomyces cerevisiae* by microarray hybridization. Mol. Biol. Cell *9*, 3273–3297.

Tai, C.Y., Dujardin, D.L., Faulkner, N.E., and Vallee, R.B. (2002). Role of dynein, dynactin, and CLIP-170 interactions in LIS1 kinetochore function. J. Cell Biol. *156*, 959–968.

Tirnauer, J.S., O'Toole, E., Berrueta, L., Bierer, B.E., and Pellman, D. (1999). Yeast Bim1p promotes the G1-specific dynamics of microtubules. J. Cell Biol. *145*, 993–1007.

Tirnauer, J.S., Canman, J.C., Salmon, E.D., and Mitchison, T.J. (2002). EB1 targets to kinetochores with attached, polymerizing microtubules. Mol. Biol. Cell *13*, 4308–4316.

Tong, A.H., Lesage, G., Bader, G.D., Ding, H., Xu, H., Xin, X., Young, J., Berriz, G.F., Brost, R.L., Chang, M., et al. (2004). Global mapping of the yeast genetic interaction network. Science *303*, 808–813.

Usui, T., Maekawa, H., Pereira, G., and Schiebel, E. (2003). The XMAP215 homologue Stu2 at yeast spindle pole bodies regulates microtubule dynamics and anchorage. EMBO J. *22*, 4779–4793.

Vogel, J., Drapkin, B., Oomen, J., Beach, D., Bloom, K., and Snyder, M. (2001). Phosphorylation of gamma-tubulin regulates microtubule organization in budding yeast. Dev. Cell *1*, 621–631.

Wang, P.J., and Huffaker, T.C. (1997). Stu2p: A microtubule-binding protein that is an essential component of the yeast spindle pole body. J. Cell Biol. *139*, 1271–1280.

Waterman-Storer, C.M., and Salmon, E.D. (1997). Actomyosin-based retrograde flow of microtubules in the lamella of migrating epithelial cells influences microtubule dynamic instability and turnover and is associated with microtubule breakage and treadmilling. J. Cell Biol. *139*, 417–434.

Yeh, E., Yang, C., Chin, E., Maddox, P., Salmon, E.D., Lew, D.J., and Bloom, K. (2000). Dynamic positioning of mitotic spindles in yeast: role of microtubule motors and cortical determinants. Mol. Biol. Cell *11*, 3949–3961.

Zhang, J., Li, S., Fischer, R., and Xiang, X. (2003). Accumulation of cytoplasmic dynein and dynactin at microtubule plus ends in *Aspergillus nidulans* is kinesin dependent. Mol. Biol. Cell *14*, 1479–1488.